

Kinetics of 2-Halopyridine Substitution at Pentaammineaquaruthenium(II)

Michael H. Schmidt,* Grady Horton, and Ilan Tong

Department of Chemistry, California State University,
San Marcos, San Marcos, California 92096-0001

Received May 26, 1998

Introduction

Work by Allen and Ford¹ and Shepherd and Taube² established that substitution at pentaammineaquaruthenium(II) proceeded by a primarily dissociative mechanism. With the exception of 2-methylpyridine and 2,6-dimethylpyridine, rate constants for various substituted pyridine ligands varied by only a factor of 2,^{1,2} with little or no obvious effect of ligand preassociation on the observed rates. However, Toma and Malin reported evidence for an unusual preassociation between the pentaammineaquaruthenium and the *N*-methylpyrazinium cation.³

We have recently studied the kinetics of 2-halopyridine substitution at $[\text{Ru}(\text{NH}_3)_5\text{H}_2\text{O}]^{2+}$ in dilute aqueous solution. In the course of these studies we discovered a previously unreported metal-catalyzed nucleophilic substitution of the halide in the case of 2-chloropyridine (2-Clpyr). Modeling of the catalytic cycle demonstrates that 2-Clpyr has a substitution rate constant that is significantly faster than rate constants for other substituted pyridines. 2-Fluoropyridine (2-Fpyr) was also found to have a higher rate constant. These results, taken with previously published rate constants, indicate that the polarity of the incoming ligand may influence the degree of outer-sphere ligand association and rate of substitution at $[\text{Ru}(\text{NH}_3)_5\text{H}_2\text{O}]^{2+}$.

Experimental Section

Kinetic Experiments. $\text{Ru}(\text{NH}_3)_5\text{Cl}_3$ and $\text{Ru}(\text{NH}_3)_5(\text{CF}_3\text{SO}_3)_3$ were synthesized from $\text{Ru}(\text{NH}_3)_6\text{Cl}_3$ according to previously published methods.^{4,5} Solutions of $[\text{Ru}(\text{NH}_3)_5\text{H}_2\text{O}]^{2+}$ were prepared by dissolving $\text{Ru}(\text{NH}_3)_5\text{Cl}_3$ in 0.1 M NaCl and sparging the solution with Ar by needle in a sealed flask. After 15–20 min, Zn/Hg amalgam was added to reduce the ruthenium species to $[\text{Ru}(\text{NH}_3)_5\text{Cl}]^+$, which spontaneously aquated to form $[\text{Ru}(\text{NH}_3)_5(\text{H}_2\text{O})]^{2+}$.

Kinetic experiments were performed in a fused quartz cuvette capped by a rubber septum. The flask was purged with Ar, and Ar-sparged solutions of $[\text{Ru}(\text{NH}_3)_5\text{H}_2\text{O}]^{2+}$ and the halopyridines in the 0.10 M NaCl solution were introduced by syringe. Typical final solution concentrations were $(0.5\text{--}1.5) \times 10^{-4}$ M ruthenium and 0.008–0.20 M ligand.

Data Analysis. Reactions of 2-Fpyr and 3-Clpyr with $[\text{Ru}(\text{NH}_3)_5\text{H}_2\text{O}]^{2+}$ were run under pseudo-first-order rate conditions and analyzed by plotting $\ln(A_\infty - A_t)$ vs time. Bimolecular rate constants were calculated by dividing these rate constants by the ligand concentration.

For reactions of 2-Clpyr with $[\text{Ru}(\text{NH}_3)_5\text{H}_2\text{O}]^{2+}$, repetitive scans within the region between 600 and 350 nm were made at intervals of 70–180 s. These spectra were deconvoluted as linear combinations of a spectrum representing $[\text{Ru}(\text{NH}_3)_5(2\text{-Clpyr})]^+$ and a spectrum representing $[\text{Ru}(\text{NH}_3)_5(2\text{-Opyr})]^+$.

Coefficients representing the relative contribution of the two basis spectra were then fit by computer to kinetic model for the reaction scheme reported below in Results. Concentrations of the observed

species were predicted using numerical fourth-order Runge–Kutta solutions⁶ of the following differential equations. In these equations, Ru(II) represents $[\text{Ru}(\text{NH}_3)_5(\text{H}_2\text{O})]^{2+}$, Ru(II)(2-Clpyr) represents $[\text{Ru}(\text{NH}_3)_5(2\text{-Clpyr})]^{2+}$, and Ru(II)(2-Opyr) represents $[\text{Ru}(\text{NH}_3)_5(2\text{-Opyr})]^+$; k_1 and k_{-1} represent the forward and reverse 2-Clpyr substitution reactions, k_2 represents the hydrolysis of the Ru-bound 2-Clpyr to form 2-Opyr, and k_3 represents the dissociation of the 2-Opyr complex.

$$d[\text{Ru(II)}]/dt = -k_1[2\text{-Clpyr}][\text{Ru(II)}] + k_{-1}[\text{Ru(II)}(2\text{-Clpyr})] + k_3[\text{Ru(II)}(2\text{-Opyr})] \quad (1)$$

$$d[\text{Ru(II)}(2\text{-Clpyr})]/dt = -k_{-1}[\text{Ru(II)}(2\text{-Clpyr})] - k_2[\text{Ru(II)}(2\text{-Clpyr})] \quad (2)$$

$$d[\text{Ru(II)}\text{Opyr}]/dt = k_2[\text{Ru(II)}(2\text{-Clpyr})] - k_3[\text{Ru(II)}(2\text{-Opyr})] \quad (3)$$

Using a simplex-based method,⁷ deconvolutions of the experimental spectra could be fit to this model using the rates of the three reactions, molar absorptivities, the elapsed time between mixing and the initial spectrum, and mixing of the $[\text{Ru}(\text{NH}_3)_5(2\text{-Clpyr})]^{2+}$ and $[\text{Ru}(\text{NH}_3)_5(2\text{-Opyr})]^+$ species in the $[\text{Ru}(\text{NH}_3)_5(2\text{-Clpyr})]^{2+}$ basis spectrum as adjustable parameters. The model was constrained by the specifying the initial concentration of $[\text{Ru}(\text{NH}_3)_5\text{H}_2\text{O}]^{2+}$ present in solution, and the concentrations of Ru complexes in the basis spectra used for deconvolution.

Analysis for 2-OHpyr. Products of the reactions of 2-Clpyr with $[\text{Ru}(\text{NH}_3)_5\text{H}_2\text{O}]^{2+}$ were subjected to ion-exchange chromatography on Dowex 50W ion-exchange resin in the Na^+ form. Elution with 0.1 M NaCl yielded a solution having a UV–visible spectrum identical to that of 2OH-pyr, and continuous extraction of this solution with dichloromethane yielded sample which was assayed for 2OH-pyr by gas chromatography/mass spectrometry.

Results

Bimolecular rate constants, k_1 , for the reaction of 2-fluoropyridine, 2-chloropyridine, and 3-chloropyridine with $[\text{Ru}(\text{NH}_3)_5\text{H}_2\text{O}]^{2+}$ are listed in Table 1. The rate of substitution with 2-bromopyridine could not be measured due to a variety of subsequent reactions (see below). The value obtained for 3-chloropyridine is substantially different than that previously reported in the literature,¹ although other published bimolecular rate constants of pyridine ligand substitution at $[\text{Ru}(\text{NH}_3)_5\text{H}_2\text{O}]^{2+}$ have been reproduced in our laboratory.

Measured activation parameters for the 2-Fpyr reaction were $\Delta H^\ddagger = 16.5 \pm 1.0$ kcal mol⁻¹ and $\Delta S^\ddagger = -7 \pm 4$ cal mol⁻¹ K⁻¹. These are within experimental error of activation parameters measured for other pyridine ligands.

Reaction with 2-Chloropyridine. As shown in Figure 1, UV-visible spectra from the reaction of 2-chloropyridine (2-Clpyr) with $[\text{Ru}(\text{NH}_3)_5\text{H}_2\text{O}]^{2+}$ show the formation of a secondary product. Final spectra could be deconvoluted into a linear combination of two basis spectra (Figure 2). One basis spectrum was that of the reaction product of 0.1 M 2-pyridine oxide (2-Opyr) with 1×10^{-4} M $[\text{Ru}(\text{NH}_3)_5\text{H}_2\text{O}]^{2+}$ in 0.10 M NaCl

- (4) Vogt, L. H.; Katz, J. L.; Wiberley, S. E. *Inorg. Chem.* **1965**, *4*, 1158–1163.
- (5) Lawrence, G. A.; Lay, P. A.; Sargeson, A. M.; Taube, H.; Englehardt, H.; Gerberhold, M. *Inorg. Synth.* **1986**, *24*, 257–261.
- (6) Mathews, J. H. *Numerical Methods for Mathematics, Science and Engineering*; Prentice Hall: Englewood Cliffs, NJ, 1987; pp 450–460.
- (7) Noggle, J. H. *Practical Curve Fitting and Data Analysis*; PTR Prentice Hall: Englewood Cliffs, NJ, 1993.

(1) Allen, R. J.; Ford, P. C. *Inorg. Chem.* **1972**, *11*, 679–685.

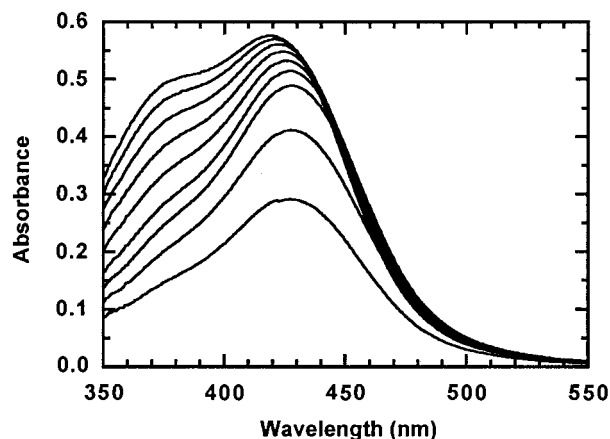
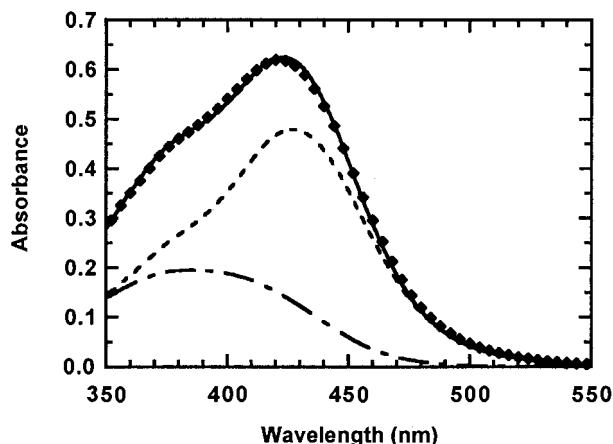
(2) Shepherd, R. E.; Taube, H. *Inorg. Chem.* **1973**, *12*, 1392–1401.

(3) Toma, H. E.; Malin, J. M. *J. Am. Chem. Soc.* **1972**, *94*, 4039–4040.

Table 1. Bimolecular Rate Constants for Substitution of Pyridine at $[\text{Ru}(\text{NH}_3)_5\text{H}_2\text{O}]^{2+}$ at 25 °C and Spectral Features of Resulting Complexes

ligand	μ , M ^a	k_1 , M ⁻¹ s ⁻¹	λ_{max} , nm	ϵ , M ⁻¹ cm ⁻¹
2-chloropyridine	0.10	0.15 ± 0.02	428	6650 ± 300
2-fluoropyridine	0.10	0.138 ± 0.009	414	6200 ± 300
3-chloropyridine	0.10	0.088 ± 0.002	427	7602 ± 300
	0.20 ^b	0.086 ± 0.002		
	0.20 ^b	0.064 ± 0.007^c		
2-pyridine oxide	—	—	389	8900 ± 300

^a Ionic strength; sodium chloride, except where noted. ^b Sodium *p*-toluenesulfonate. ^c Reference 2.

**Figure 1.** Selected spectra from the reaction of 1.1×10^{-4} M $[\text{Ru}(\text{NH}_3)_5\text{H}_2\text{O}]^{2+}$ with 0.0512 M 2-chloropyridine at 25.0 °C. The initial spectrum after mixing is at the bottom; subsequent spectral scans were started 90, 270, 630, 1350, 2160, 3150, 4500, and 6300 s after the initial spectral scan was started.**Figure 2.** Linear deconvolution of a spectrum taken approximately 3510 s into the reaction of 1.7×10^{-4} M $[\text{Ru}(\text{NH}_3)_5\text{H}_2\text{O}]^{2+}$ with 0.0167 M 2-chloropyridine at 25 °C: (—) data; (◆) fit; (---) component of fit primarily due to $[\text{Ru}(\text{NH}_3)_5(2\text{-Clpyr})]^{2+}$; (- - -) component of fit due to $[\text{Ru}(\text{NH}_3)_5(2\text{-Opyr})]^+$.

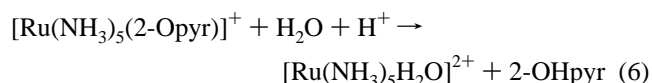
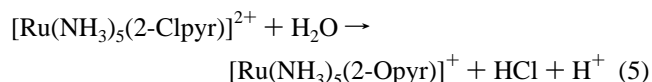
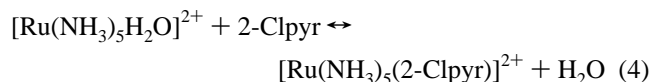
buffered at pH 10. The other basis spectrum was taken from a reaction between 2-Clpyr and $[\text{Ru}(\text{NH}_3)_5\text{H}_2\text{O}]^{2+}$. The product of the reaction of 2-Opyr⁻ and $[\text{Ru}(\text{NH}_3)_5\text{H}_2\text{O}]^{2+}$, having a broad absorption centered around 389 nm, was presumed to be $[\text{Ru}(\text{NH}_3)_5(2\text{-Opyr})]^+$.

The relative stability of the putative $[\text{Ru}(\text{NH}_3)_5(2\text{-Opyr})]^+$ in pH 10 buffer supports the assignment of this species as the ruthenium complex of the deprotonated ligand; in pH 9 and pH 8 buffers, the complex decomposes. Additionally, the complex elutes from Dowex 50W ion-exchange resin at lower salt concentrations than those required for elution of dipositive

ruthenium–pyridine complexes, supporting the assignment of this complex as $[\text{Ru}(\text{NH}_3)_5(2\text{-Opyr})]^+$.

When samples of a crude preparation of the hexafluorophosphate salt of $[\text{Ru}(\text{NH}_3)_5(2\text{-Opyr})]^+$ were dissolved in a solution of 0.1 mM isonicotinamide, the UV–visible spectrum displayed a prominent peak at 480 nm, indicating formation of the $[\text{Ru}(\text{NH}_3)_5(\text{isonicotinamide})]^{2+}$ complex.⁸ This suggested that the $[\text{Ru}(\text{NH}_3)_5(2\text{-Opyr})]^+$ complex easily hydrolyzed to form $[\text{Ru}(\text{NH}_3)_5\text{H}_2\text{O}]^{2+}$, with subsequent substitution of water by isonicotinamide.

The facile hydrolysis of the $[\text{Ru}(\text{NH}_3)_5(2\text{-Opyr})]^+$ complex suggested the following catalytic cycle for the conversion of 2-chloropyridine to 2-OHpyr:



Ion chromatography and dichloromethane extraction of reactions of $[\text{Ru}(\text{NH}_3)_5\text{H}_2\text{O}]^{2+}$ with 2-Clpyr yielded ultraviolet spectra and GC/MS evidence of the production of 2-OHpyr. The difficulty of obtaining quantitative recovery through the ion-exchange and extraction steps prevented the quantitation of 2-OHpyr. The drop in pH expected in unbuffered solution predicted by eq 5 was not observed, with final pH values after several hours of reaction typically yielding pH values of 8.4–8.8. This may have been the result of decomposing $\text{Ru}(\text{NH}_3)_5$ moieties releasing significant quantities of NH_3 into solution, effectively buffering the pH at higher levels.

The coefficients obtained from the spectrum deconvolution described above could be fit to a kinetic model of the above catalytic scheme, as shown in Figure 3. The bimolecular rate constant k_1 for 2-chloropyridine substitution reported in Table 1 is the average of the best fit to the kinetic model of three data sets taken at different ligand concentrations.

The rate constant for nucleophilic substitution at the 2-chloropyridine ligand was found from these fits to be $(1.5 \pm 0.5) \times 10^{-4}$ s⁻¹ at 25 °C. The fitted rate constant for the decomposition of $[\text{Ru}(\text{NH}_3)_5(2\text{-Opyr})]^+$ was found to be $(1.8 \pm 0.5) \times 10^{-4}$ s⁻¹.

Reaction with 2-Bromopyridine. The reaction of 2-bromopyridine with $[\text{Ru}(\text{NH}_3)_5\text{H}_2\text{O}]^{2+}$ appeared to yield an initial product having an absorption maximum near 430 nm. As with the 2-chloropyridine, subsequent reactions change the UV–visible spectrum as the reaction proceeds, but $[\text{Ru}(\text{NH}_3)_5(2\text{-Opyr})]^+$ did not appear to be the only product in this case.

Discussion

Implications of Ligand Substitution Rates. Previously, no neutral pyridine ligands had published rate constants greater than that of isonicotinamide at $0.105 \text{ M}^{-1} \text{ s}^{-1}$.^{1,2} Pyridines such as 2-methylpyridine and 2,6-dimethylpyridine had very low substitution rate constants, which was attributed to steric hindrance of the ortho substituents. In this work, we found substitution rate constants significantly greater than those of other substituted

(8) Ford, P.; Rudd, D. F. P.; Gaunder, R.; Taube, H. *J. Am. Chem. Soc.* **1968**, *90*, 1187.

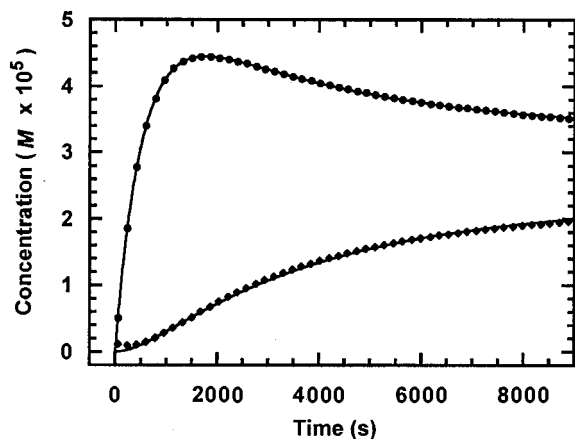


Figure 3. Fitted concentrations of $[\text{Ru}(\text{NH}_3)_5(2\text{-Clpyr})]^{2+}$ and $[\text{Ru}(\text{NH}_3)_5(2\text{-Opyr})]^+$ as a function of time for the reaction of 7.0×10^{-5} M $[\text{Ru}(\text{NH}_3)_5\text{H}_2\text{O}]^{2+}$ with 0.0087 M 2-chloropyridine at 25.0 °C: (●) concentrations of $[\text{Ru}(\text{NH}_3)_5(2\text{-Clpyr})]^{2+}$ derived from deconvoluted spectra using molar absorptivities obtained from the fitting routine; (◆) concentrations of $[\text{Ru}(\text{NH}_3)_5(2\text{-Opyr})]^+$ derived from deconvoluted spectra using molar absorptivities obtained from the fitting routine; (—) modeled concentrations of $[\text{Ru}(\text{NH}_3)_5(2\text{-Clpyr})]^{2+}$ and $[\text{Ru}(\text{NH}_3)_5(2\text{-Opyr})]^+$. Every second data point omitted for clarity.

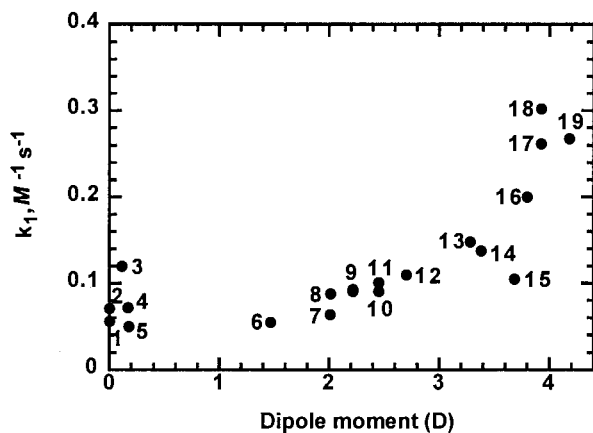


Figure 4. Plot of bimolecular rate constants, k_1 , as a function of dipole moment. All rate constants were determined in 0.10 M LiCl or NaCl except where noted: 1 = pyrazine (ref 2); 2 = N_2 (ref 2); 3 = CO (ref 2); 4 = N_2O (ref 2); 5 = 2-methylpyrazine (ref 2); 6 = NH_3 (ref 2); 7 = 3-chloropyridine, (ref 1, 0.20 M sodium *p*-toluenesulfonate); 8 = 3-chloropyridine (this work); 9 = pyridine (refs 1 and 2); 10 = 3-methylpyridine (ref 1, 0.20 M sodium *p*-toluenesulfonate); 11 = 3-methylpyridine (ref 2); 12 = 4-methylpyridine (ref 1, 0.20 M sodium *p*-toluenesulfonate); 13 = 2-chloropyridine (this work); 14 = 2-fluoropyridine (this work); 15 = isonicotinamide (ref 2); 16 = imidazole (ref 2); 17 = acetonitrile (ref 1; $\mu \approx 1 \times 10^{-4}$); 18 = acetonitrile (ref 2); 19 = benzonitrile (ref 1; 0.20 M sodium *p*-toluenesulfonate). Dipole moments from ref 15 and references therein.

pyridines despite ortho substitution. This new data, when combined with previously published data, suggests a correlation between electric dipole moment and the substitution rate. Figure 4 shows a plot of the bimolecular rate constants, k_1 , for a variety of ligands as a function of experimental dipole moments.⁹ With the exception of CO, rate constants are quite similar for ligands with dipole moments less than that of water. Rate constants increase for ligands with moments above 2 D, with the exception of isonicotinamide.

(9) (a) McClellan, A. L. *Tables of Experimental Dipole Moments*; W. H. Freeman and Company: San Francisco, 1963. (b) McClellan, A. L. *Tables of Experimental Dipole Moments*; Rahara Enterprises: El Cerrito, CA, 1974; Vol. 2. (c) McClellan, A. L. *Tables of Experimental Dipole Moments*; Rahara Enterprises: El Cerrito, CA, 1989; Vol. 3.

The Eigen–Wilkins mechanism for ligand substitution at transition metal complexes¹⁰ postulates an initial outer-sphere binding step characterized by the equilibrium constant K_{OS} , a rate-determining dissociation of the H_2O , and a subsequent rapid binding of the incoming ligand L. These last two steps are often reduced to a single interchange step characterized by the rate constant k_i .¹¹

The resulting overall rate expression for the ligand exchange is

$$\begin{aligned} d[\text{Ru}(\text{NH}_3)_5\text{L}^{2+}]/dt &= K_{\text{OS}}k_i[\text{Ru}(\text{NH}_3)_5\text{H}_2\text{O}^{2+}][\text{L}]/(1 + K_{\text{OS}}[\text{L}]) \\ &= k_1[\text{Ru}(\text{NH}_3)_5\text{H}_2\text{O}^{2+}][\text{L}] \end{aligned}$$

As long as $K_{\text{OS}}[\text{L}]$ is significantly less than 1, this reduces to

$$k_1 = K_{\text{OS}}k_i$$

In the context of this mechanism, the observed increase in k_1 for ligands with electric dipole moments greater than that of water can be attributed to an increase in K_{OS} with increasing ligand polarity. K_{OS} is often estimated using a variant the Fuoss equation¹² adapted for nonionic ligands.¹³ This equation does not take into account the polarity of the ligands, which may be a justified simplification if the ligand dipole moments are less than or equal to that of the solvent water.¹³ The correlation noted above invites development of a more detailed theory for K_{OS} which can account for the effect of greater ligand polarity.

The orientation of the dipole may also affect the rate as the dipole strength increases; this may explain why isonicotinamide does not fit the general correlation between rate constant and dipole moment.

Catalysis of Nucleophilic Substitution. Catalysis of nucleophilic substitution at pyridine by copper and zinc has been previously observed, although previous studies have involved aminolysis in 20% ammonia or anhydrous ammonia at temperatures of 180–220 °C.¹⁴ Typically, hydrolysis of 2-chloropyridine requires strongly acidic or basic conditions at elevated temperatures to proceed; in our laboratory, hydrolysis in dilute aqueous conditions similar to those used in the ruthenium-complex studies was minimal over several days of reaction in 1 M NaOH at 100 °C.

The ease of nucleophilic substitution at the 2 and 4 position of pyridine has been traditionally explained as the result of a $\text{S}_{\text{N}}2$ transition state stabilized by localization of a second lone pair of electrons on the ring nitrogen.¹⁵ Such a transition state gives the nitrogen a negative formal charge, which would be stabilized by sigma donation to the dipositive ruthenium center. We cannot at the present time rule out steric and hydrogen-bonding interactions with the Ru-bound ammine ligands, or more specific electronic effects of metal d electrons.

Conclusion

A survey of the reaction of 2-halopyridines at pentaammineaquaruthenium has shown these ligands to have a range

(10) Eigen, M.; Wilkins, R. G. *Adv. Chem. Ser.* **1965**, 49, 55–80.

(11) Burgess, J. *Metal Ions in Solution*; Ellis Horwood Ltd.: Chichester, 1978; pp 350–416.

(12) Fuoss, R. M. *J. Am. Chem. Soc.* **1958**, 80, 5059–5061.

(13) Rorabacher, D. B. *Inorg. Chem.* **1966**, 5, 1891–1899.

(14) (a) Wibaut, J. P.; Nicolai, J. R. *Rec. Trav. Chim.* **1939**, 58, 709–721. (b) Fischer, O. *Ber. Dtsch. Chem. Ges.* **1899**, 32, 1297.

(15) Kemp, D. S.; Vellaccio, F. *Organic Chemistry*; Worth Publishers: New York, 1980; 1236. (b) Davies, D. I. *Aromatic Heterocyclic Chemistry*; Oxford University Press: Oxford, 1992.

of substitution rates beyond those previously observed for substituted pyridines. These rates, and those of other ligands, correlate with the dipole moments of the ligands, suggesting an effect of ligand polarity on the equilibria for outer-sphere complex formation. Additionally, ruthenium-catalyzed nucleophilic substitution of 2-chloropyridine has been observed.

Acknowledgment is made to the donors of the Petroleum Research Fund, administered by the American Chemical Society, for support of this research via Grant No. 28205-GB3. Ac-

knowledgment is also made to Dr. Paul Jasien for review of the manuscript and to Prof. Albert Haim and the reviewers for helpful comments.

Supporting Information Available: An expanded Experimental Section detailing the kinetic experiments, their analysis, and the synthesis of $[\text{Ru}(\text{NH}_3)_5(2\text{-Opyr})]\text{PF}_6$ is available (7 pages). Ordering information is given on any current masthead page.

IC980584U